

Breakup of the doubly magic ^{100}Sn core

M. Lipoglavšek,^{1,2} C. Baktash,¹ J. Blomqvist,³ M. P. Carpenter,⁴ D. J. Dean,¹ T. Engeland,⁵ C. Fahlander,⁶ M. Hjorth-Jensen,⁵ R. V. F. Janssens,⁴ A. Likar,² J. Nyberg,⁷ E. Osnes,⁵ S. D. Paul,¹ A. Piechaczek,⁸ D. C. Radford,¹ D. Rudolph,⁶ D. Seweryniak,⁴ D. G. Sarantites,⁹ M. Vencelj,² and C.-H. Yu¹

¹Physics Division, Oak Ridge National Laboratory, Oak Ridge, Tennessee 37831-6371

²J. Stefan Institute, Ljubljana, Slovenia

³Department of Physics, Royal Institute of Technology, Stockholm, Sweden

⁴Argonne National Laboratory, Argonne, Illinois 60439

⁵Department of Physics, University of Oslo, Oslo, Norway

⁶Department of Physics, Lund University, Lund, Sweden

⁷Department of Neutron Research, Uppsala University, Uppsala, Sweden

⁸Louisiana State University, Baton Rouge, Louisiana 70803

⁹Department of Chemistry, Washington University, St. Louis, Missouri 63130

(Received 8 January 2002; published 26 July 2002)

Level schemes of $^{99}\text{Cd}_{51}$ and $^{101}\text{In}_{52}$ nuclei have been extended to high spin. The breakup of the doubly magic ^{100}Sn core has been observed. Large-scale shell model calculations based on realistic nucleon-nucleon interactions are in good agreement with the experimental data. These results provide a reliable basis to predict nuclear structure properties in ^{100}Sn and its neighbors. For example, the size of the $N=50$ shell gap and the energy of the first excited state in ^{101}Sn have been deduced.

DOI: 10.1103/PhysRevC.66.011302

PACS number(s): 21.10.-k, 21.60.Cs, 23.20.Lv, 27.60.+j

Doubly magic nuclei and their immediate neighbors are of great interest as they provide direct information on the basic shell structure that is ultimately responsible for most nuclear properties. Lying at the proton drip line and being the heaviest particle-stable, self-conjugate nucleus, ^{100}Sn is particularly relevant in this context. An important property of this nucleus is the degree of rigidity of its spherical shape which is reflected in the excitation energy of the lowest 2^+ state and in the associated $B(E2; 2^+ \rightarrow 0^+)$ transition rate. The main component of the wave function of this level in a microscopic description is presumably an isoscalar mixture of proton and neutron $2d_{5/2}1g_{9/2}^{-1}$ excitations across the $N=Z=50$ shell gaps. This state is at present not known experimentally and its observation may well require the availability of intense exotic beams. Some guidance about its excitation energy can perhaps come from other doubly magic nuclei. In the $N=Z=28$ doubly magic nucleus, the first 2^+ state is located rather low, at 2.7 MeV. In contrast, the 2^+ levels in ^{132}Sn and ^{208}Pb are much higher in excitation energy, 4.0 and 4.1 MeV, respectively, and in the latter nucleus the size of the shell gaps can also be appreciated from the fact that this state is not even the lowest excitation, but instead lies above a 3^- (octupole) vibrational state.

In order to estimate the position of the 2^+ state in ^{100}Sn , both proton and neutron shell gaps have to be known [1]. The energy splittings of the relevant single-particle orbitals in the other heavy doubly magic nuclei are comparable. The neutron $2p_{3/2}$ and $1f_{7/2}$ orbitals are 6.4 MeV apart in ^{56}Ni , while the splittings between the $2f_{7/2}$ and $1h_{11/2}$ levels in ^{132}Sn and $2g_{9/2}$ and $1i_{13/2}$ states in ^{208}Pb are 4.9 and 5.1 MeV, respectively. Here, the splitting between the $2d_{5/2}$ and $1g_{9/2}$ neutron orbits will be shown to be of the order of 6 MeV as in the ^{56}Ni case. However, a sizable proton-neutron interaction could, as in ^{56}Ni , decrease the excitation energy

and increase the transition rate for the lowest 2^+ state in ^{100}Sn . Such an interaction is expected to be especially strong in $N=Z$ nuclei, where protons and neutrons occupy the same single-particle orbitals, which results in a large spatial overlap of their wave functions. In this paper, we address a number of similarities between nuclei near ^{56}Ni and ^{100}Sn , including the sizes of the neutron shell gaps and the positions of the core-excited states in the $T_z=3/2$ nuclei. Some of them have already been discussed elsewhere, see e.g., Ref. [2]. To interpret the level schemes obtained in the experiment, we performed large-scale shell model calculations using effective interactions based on CD-Bonn nucleon-nucleon interaction.

Nuclei near ^{100}Sn were studied using the $^{58}\text{Ni}+^{50}\text{Cr}$ reaction. A ^{58}Ni beam of 225 MeV was provided by the ATLAS superconducting linear accelerator at Argonne National Laboratory. The ^{50}Cr target had a thickness of 2.1 mg/cm² and was isotopically enriched to better than 99%. It was backed by 10 mg/cm² Au in order to stop the residual nuclei. The experimental setup consisted of the GAMMASPHERE array [3], comprising 78 Compton-suppressed Ge detectors, augmented by the Microball [4], a 4π array of 95 CsI scintillators for light charged particle detection, and the Neutron Shell [5], an array of 30 liquid scintillator detectors. Neutron detectors covered a solid angle of about 1π in the forward direction. The average detection and identification efficiencies for protons, α particles, and neutrons were 78%, 47%, and 27%, respectively. In the offline analysis, events were sorted into a variety of γ -ray spectra and γ - γ coincidence matrices that were gated by the appropriate number of neutrons and charged particles to select the exit channels of interest. The partial cross sections for ^{99}Cd and ^{101}In were found to be 0.01% and 0.02% of the total evaporation residue cross section. Further experimental details are given in Ref. [6].

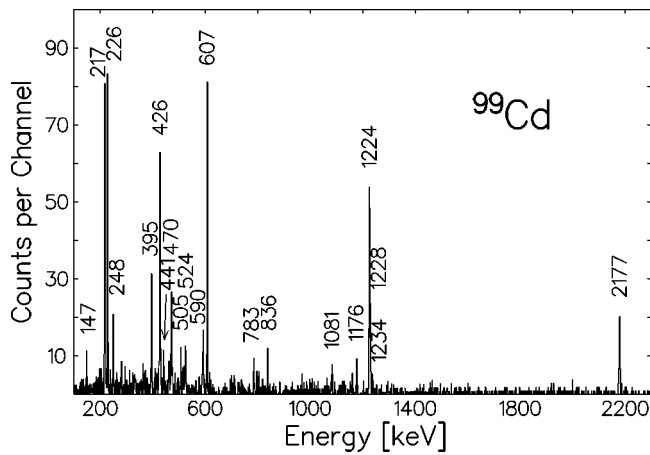


FIG. 1. A γ - γ coincidence spectrum for ^{99}Cd obtained by requiring a coincidence between one neutron, two α particles, and the 226, 607, or 1224 keV γ rays.

A partial level scheme for ^{99}Cd comprising six γ rays with energies of 217, 226, 395, 426, 607, and 1224 keV has been reported in the literature [7]. In the present experiment, all these γ rays were also observed in the γ -ray spectrum corresponding to ^{99}Cd residues, which was generated by requiring the coincident detection of two α particles and one neutron. Furthermore, γ - γ coincidence data were used to identify many new γ rays in ^{99}Cd (see Fig. 1); these were placed in the partial level scheme presented in Fig. 2. All γ rays assigned to ^{99}Cd are listed in Table I, together with their intensities and angular distribution coefficients A_2 and A_4 [8]. As an example, the angular distribution of the 2177 keV γ ray is shown in Fig. 3, which shows that the 2177 keV transition is most likely of quadrupole character. Multipolarity assignments for the γ rays were deduced from the measured angular distributions, assuming stretched dipole, quadrupole and mixed $M1/E2$ transitions. Stretched dipole transitions have negative A_2 coefficients and $A_4=0$, while

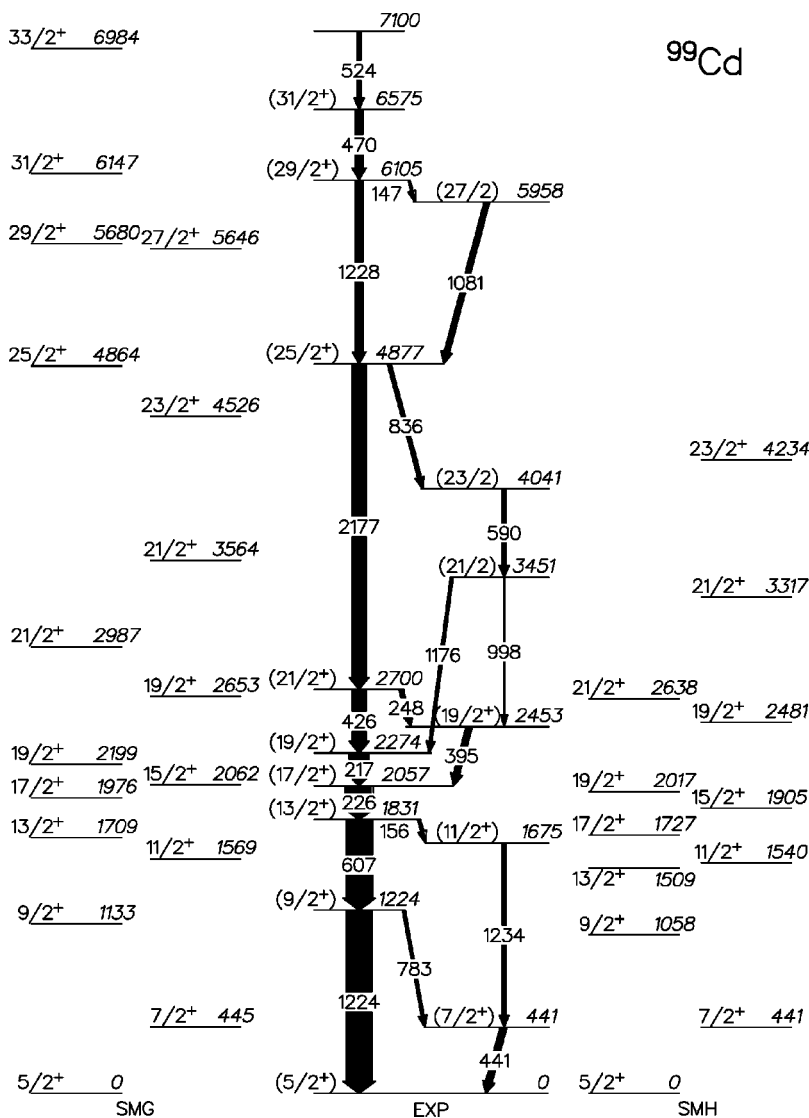


FIG. 2. Experimental (EXP) and calculated (SMH, SMG) level schemes for ^{99}Cd . The widths of the arrows are proportional to the intensities of the γ rays observed in the experiment. As discussed in the text, the $(25/2^+)$ and higher-lying states require excitations across the ^{100}Sn core.

TABLE I. Energies, relative γ -ray intensities, and angular distribution coefficients for γ rays assigned to ^{99}Cd .

Energy (keV)	Relative intensity	Angular distribution coefficients	
		A_2	A_4
146.8(5)	6(2)		
156.4(4)	8(1)		
216.8(3)	57(3)	0.2(2)	
226.3(2)	81(3)	0.39(9)	-0.1(1)
247.8(3)	13(1)	-0.2(2)	
395.0(3)	19(1)	-0.4(2)	
426.1(2)	42(2)	-0.29(4)	0.16(5)
440.7(3)	20(1)	0.2(3)	0.1(3)
470.1(3)	24(1)	-0.3(1)	
505.4(5)	6(3)		
524.1(4)	13(2)		
590.1(4)	14(1)	-0.2(2)	
606.9(2)	81(3)	0.29(7)	-0.14(9)
783.1(7)	9(2)		
836.1(4)	11(2)	0.1(4)	
998(1)	4(2)		
1081.2(3)	16(1)	-0.1(3)	
1176.3(4)	9(1)		
1224.4(3)	80(3)	0.24(8)	-0.1(1)
1228.3(3)	23(2)	0.5(3)	-0.1(4)
1234.1(4)	11(1)	0.4(3)	
2177.1(3)	42(3)	0.3(1)	-0.1(2)

for stretched quadrupole transitions $A_2 > 0$ and $A_4 < 0$. Mixed $M1/E2$ transitions do not fulfill the above criteria. The ground state quantum numbers were adopted from Ref. [7]. As these remain uncertain, all quantum numbers in the level scheme are tentative. The angular momentum quantum number assignments are made in rising order with excitation energies. The $17/2^+$ level in ^{99}Cd is isomeric and its lifetime will be discussed at length in a forthcoming paper [9].

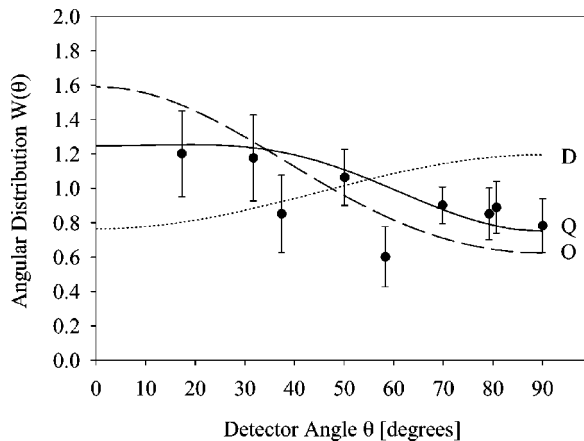


FIG. 3. Experimental angular distribution of the 2177 keV γ ray in ^{99}Cd compared to calculated distributions [8] of the final transitions in the $29/2^- \rightarrow 27/2^- \rightarrow 23/2^- \rightarrow 21/2$ (D), $31/2^- \rightarrow 29/2^- \rightarrow 25/2^- \rightarrow 21/2$ (Q), and $33/2^- \rightarrow 31/2^- \rightarrow 27/2^- \rightarrow 21/2$ (O) cascades. The initial states are assumed to be completely aligned in all three cases.

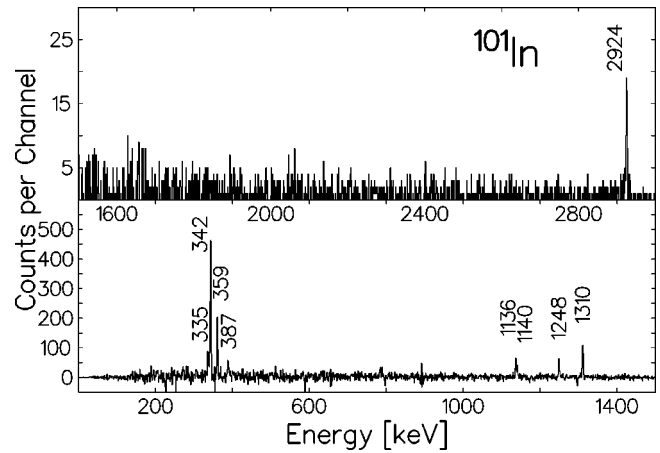


FIG. 4. A representative γ - γ coincidence spectrum for ^{101}In obtained by requiring one proton, one α particle, one or two neutrons, and 359 or 1310 keV γ rays in coincidence.

In the reaction used, the $1p1\alpha2n$ evaporation channel leads to ^{101}In . Prior to this work, only a single 1310 keV γ ray had been assigned to this nucleus [10]. Hence, γ rays detected in coincidence with one proton, one α particle, and one or two neutrons have been carefully investigated. In addition to the 1310 keV line, this particle-gated spectrum revealed eight additional transitions that were found to be in coincidence with the latter γ ray, as seen in Fig. 4. The partial level scheme for ^{101}In , shown in Fig. 5, was constructed using a procedure similar to the one described above for ^{99}Cd . ^{101}In γ rays are listed in Table II, together with their intensities and angular distribution coefficients A_2 . The J^π assignments to the 3295, 4395, and 4782 keV states are primarily based on the systematics of heavier indium isotopes [11]. No isomeric states have been observed in ^{101}In inside the experimental time window between 2 ns and 1 μs .

Large-scale shell model calculations helped to interpret obtained level schemes. In the first calculation, ^{88}Sr was taken as the closed shell core and an effective interaction based on the CD-Bonn nucleon-nucleon interaction was used [12]. The effective two-body interactions were applied in a shell-model space spanning $2s_{1/2}$, $1d_{5/2}$, $1d_{3/2}$, $0g_{7/2}$, and $0h_{11/2}$ neutron, and $0g_{9/2}$ and $1p_{1/2}$ proton single-particle orbitals [13]. Reference [14] describes how the effective interaction for nuclei near $A \sim 100$ was derived. In this model space, ^{99}Cd has one neutron and ten protons outside the core. The results of the calculation, denoted as SMH, are compared with the experimental levels in Fig. 2. The calculation favors a $J^\pi = 5/2^+$ assignment for the ground state, in agreement with the systematics of odd- A , $N=51$ isotones. The wave functions of the states with $J^\pi = 5/2^+$, $9/2^+$, $13/2^+$, $17/2^+$, $19/2_1^+$, and $21/2_1^+$ all have main configurations where the valence neutron is in the $d_{5/2}$ orbit, while the $7/2^+$, $11/2^+$, $15/2^+$, $19/2_2^+$, $21/2_2^+$, and $23/2^+$ levels are associated with the predominant occupation of the $g_{7/2}$ orbit. For all these states, the two proton holes always remain assigned to the $g_{9/2}$ orbit. The lowest $7/2^+$ states in $N=51$ isotones from ^{91}Zr to ^{97}Pd are well reproduced by using the experi-

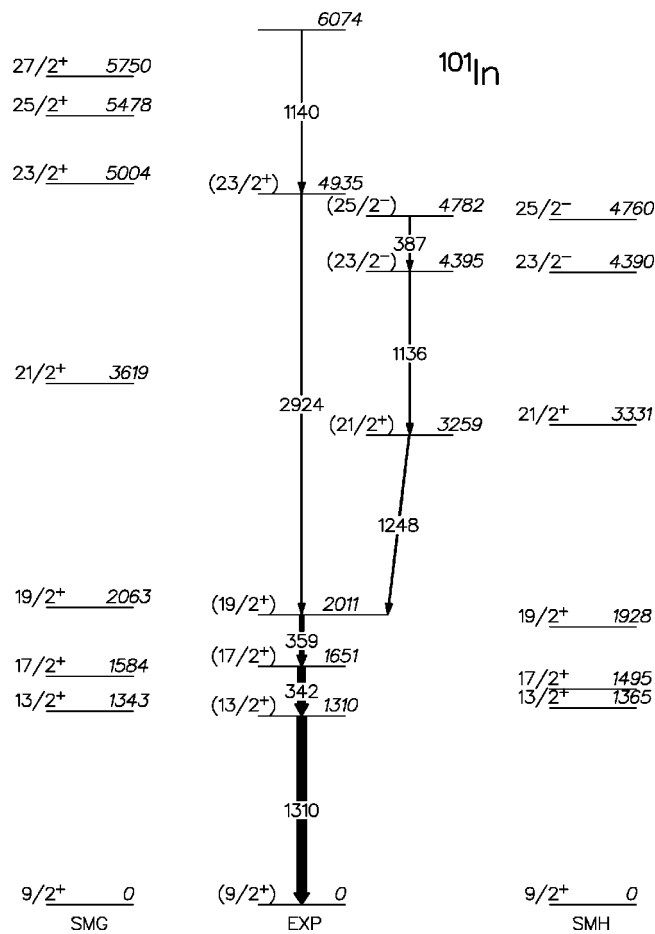


FIG. 5. Experimental (EXP) and calculated (SMH, SMG) level schemes for ^{101}In . The widths of the arrows are proportional to the intensities of the γ rays observed in the experiment. The $(23/2^+)$ state requires excitations across the ^{100}Sn core.

mental $g_{7/2}$ single-particle energy from zirconium [13], but in ^{99}Cd this state was calculated 250 keV too low. Therefore, the single-particle energy of the neutron $g_{7/2}$ orbit, relative to the ^{88}Sr core was increased from 2.63 to 2.89 MeV in order to reproduce the experimental excitation energy of the $7/2^+$ state. This yielded excellent agreement between calculations and experiment up to the $J^\pi = 23/2^+$ state (Fig. 2), the highest spin that can be generated in this model space for positive-parity states in ^{99}Cd . The description of higher-spin states requires the excitation of one or more $g_{9/2}$ particles across the $N, Z = 50$ shell gaps, an excitation similar to that responsible for the first 2^+ and higher-lying states in ^{100}Sn .

To study the high-spin states, another shell-model calculation was performed using this time ^{78}Sr as a closed shell core. The results are denoted as SMG in Fig. 2. The same model space as in the previous calculation was employed except for the $h_{11/2}$ neutron orbit which was replaced by the $g_{9/2}$ one. (Since this $h_{11/2}$ state lies at a relatively high excitation energy, its contribution to the positive-parity states is small.) Due to limitations in computing time, only up to two neutrons were allowed to leave the $g_{9/2}$ orbit. (Note that the $g_{9/2}$ orbit lies below the $N = 50$ shell gap, while all other neutron orbitals in this model space lie above this gap.)

TABLE II. Energies, relative γ -ray intensities, and A_2 angular distribution coefficients for γ rays assigned to ^{101}In .

Energy (keV)	Relative intensity	Angular distribution parameter A_2
334.9(5)	9(2)	
341.8(2)	94(5)	0.2(1)
359.4(3)	51(3)	-0.4(2)
386.8(5)	8(2)	
1136(1)	14(5)	
1139.6(7)	10(3)	
1247.9(4)	14(2)	-0.2(3)
1309.7(3)	100(10)	0.3(1)
2923.6(5)	11(3)	0.4(2)

Opening of the $N = 50$ shell only is justified since a neutron hole in the $g_{9/2}$ orbit, together with an existing proton hole, produces a very attractive 9^+ proton-neutron coupling. Similarly, the excited neutron, together with the one already occupying the same orbit, produces a 0^+ neutron pair with a strong attractive interaction. Opening the $Z = 50$ shell would not result in such a strong attraction. Single-particle energies with respect to the ^{78}Sr core are not known and were kept the same as in Ref. [13] for the ^{88}Sr core. The energy of the $g_{9/2}$ orbit was placed 5.0 MeV below that of the $d_{5/2}$ state. The wave functions of the states below the $25/2^+$ level are very similar to those obtained in the SMH calculation (which assumed that the $g_{9/2}$ neutron orbit is completely filled), except for the two $19/2^+$ levels, where the occupation numbers are reversed for the $d_{5/2}$ and $g_{7/2}$ orbits. The $25/2^+$ level and the higher-lying states have nine neutrons in the $g_{9/2}$ orbit with the remaining neutron pair almost evenly distributed over the $d_{5/2}$ and $g_{7/2}$ orbits. These states, therefore, represent the breakup of the doubly magic ^{100}Sn core. Thus, the excitation energy of the states with $J^\pi \geq 25/2^+$ is sensitive to the position of the $g_{9/2}$ orbit. By fitting this single-particle energy to 5.0 MeV we, therefore, indirectly deduced the size of the $N = 50$ shell gap to be 6.5 MeV as defined by $2\text{BE}(^{100}\text{Sn}) - \text{BE}(^{99}\text{Sn}) - \text{BE}(^{101}\text{Sn})$, where BE stands for binding energy. This value agrees well with earlier predictions from Hartree-Fock calculations by Leander *et al.* [15], as well as a single-particle energy parametrization by Duflo and Zuker [16] and an extrapolation by Grawe *et al.* [2]. To investigate the effect of the truncation of the model space on the deduced size of the $N = 50$ shell gap we calculated the excitation energy of the $J^\pi = 25/2^+$ state in ^{99}Cd using two different model spaces. In the first one, we allowed up to four neutrons to leave the $g_{9/2}$ orbit and the second truncation scheme restricted the valence particles to only two in each active orbit. Different truncations of the model space required adjustments of the $g_{9/2}$ single-particle energy to reproduce the experimental excitation energy of the $25/2^+$ level, but when this was achieved the size of the $N = 50$ shell gap remained within 0.5 MeV of the above value. This illustrates a relative insensitivity of our inferred result to the truncation procedure used in the shell model calculation.

Calculations using the same single-particle energies and

matrix elements were also performed for ^{101}In , which has one proton hole and two neutrons outside the $N=Z=50$ doubly closed shells. Again, the results, labeled as SMH and SMG, are in very good agreement with the experimental level scheme (Fig. 4). In these calculations, the proton hole remains in the $g_{9/2}$ orbital and a $J^\pi=9/2^+$ assignment follows for the ground state. This is in agreement with the systematics of odd- A In isotopes. The valence neutron pair is distributed over the $d_{5/2}$ and $g_{7/2}$ orbits for the ground state, while it occupies predominantly the $d_{5/2}$ state for the $13/2^+$ level. One neutron is promoted to the $g_{7/2}$ and $h_{11/2}$ orbitals to generate the $17/2^+$, $19/2^+$, $21/2^+$ positive-parity, and $23/2^-$, $25/2^-$ negative-parity states, respectively. The large separation between the $19/2^+$ and $21/2^+$ states, which are associated with the same dominant configuration, is attributed to the strong repulsion between the aligned $g_{9/2}$ proton hole and the $g_{7/2}$ neutron. Note that the $\pi g_{9/2} \nu h_{11/2}$ matrix elements used to calculate the negative-parity states in ^{102}In described in Ref. [17] were adopted here as well. The maximum spin that can be reached with the $\pi g_{9/2} \nu d_{5/2} g_{7/2}$ configuration is $21/2$. Excitation of one or more particles across the $N, Z=50$ shell gaps is again needed to account for the positive-parity states of higher spin. Thus, the $23/2^+$ level is the lowest-lying core-excited state in ^{101}In . The calculated energy gap of 2941 keV between the $23/2^+$ and $19/2^+$ states is in excellent agreement with the experimental value of 2924 keV. Experimentally known lowest lying core excited states were also calculated in the nuclei ^{98}Ag [9] and ^{96}Pd [18] using the SMG model space. Their excitation energies were reproduced to better than 100 keV. It would also be of interest to identify core excited states in nuclei near ^{90}Zr ($Z=40$, $N=50$). Unfortunately, this is more difficult because in these nuclei high-spin states can be easily reached by promoting a pair of protons from the low-spin $p_{1/2}$ orbit into the empty $g_{9/2}$ orbit.

The interactions used in these SMH and SMG calculations were also applied to a shell model calculation of the lowest-lying levels in ^{101}Sn . Both SMH and SMG calculations favor $J^\pi=5/2^+$ quantum numbers for the ground state, while the $7/2^+$ state lies only ~ 100 keV above it. This is in excellent agreement with the extrapolated energy deduced from the systematics of odd- A Sn isotopes down to ^{103}Sn [19].

It is also worth pointing out that the level schemes of ^{99}Cd and ^{101}In closely mirror those of their analogs in the ^{56}Ni region; i.e., ^{55}Fe [20] and ^{57}Co [21]. In particular, the lowest-lying core-excited states have almost identical excitation energies. This observation, together with the deduced $N=50$ shell gap, again points to a large similarity between the two heaviest self-conjugated doubly magic nuclei and one may conclude that the lowest 2^+ states in ^{56}Ni and ^{100}Sn would have closely related excitation energies if the sizes of the $Z=28$ and $Z=50$ shell gaps were also similar.

In summary, several core-excited states were identified in the $T_z=3/2$ nuclei $^{99}\text{Cd}_{51}$ and $^{101}\text{In}_{52}$, with three active particles outside the doubly magic nucleus ^{100}Sn . Results of large-scale shell model calculations based on realistic nucleon-nucleon interactions are in good agreement with the experimental data. These results confirm the long-predicted close similarity between the core-excited states in and near the two heaviest doubly magic self-conjugate nuclei ^{56}Ni and ^{100}Sn . Therefore, they provide a reliable basis to predict nuclear structure properties in ^{100}Sn and its neighbors.

Oak Ridge National Laboratory is operated by UT-Battelle, LLC for the U.S. Department of Energy under Contract No. DE-AC05-00OR22725. Work at Argonne National Laboratory is supported by the U.S. Department of Energy under Contract No. W-31-109-ENG-38 and at Washington University under Contract No. DE-FG02-88ER40406. This work was supported in part by the Swedish Natural Science Research Council.

-
- [1] I.P. Johnstone and L.D. Skouras, *J. Phys. G* **21**, L63 (1995).
 [2] H. Grawe *et al.*, in *Proceedings of the 6th International Seminar Highlights of Modern Nuclear Structure*, edited by A. Covello (World Scientific, Singapore, 1999), p. 137.
 [3] I.Y. Lee, *Nucl. Phys.* **A520**, 641c (1990).
 [4] D.G. Sarantites *et al.*, *Nucl. Instrum. Methods Phys. Res. A* **381**, 418 (1996).
 [5] D.G. Sarantites (unpublished); <http://wunmr.wustl.edu/dgs/NeutronShell/NeutronShell.html>
 [6] M. Lipoglavšek *et al.*, *Nucl. Phys.* **A682**, 399c (2001).
 [7] M. Lipoglavšek *et al.*, *Phys. Rev. Lett.* **76**, 888 (1996).
 [8] T. Yamazaki, *Nucl. Data, Sect. A* **3**, 1 (1967).
 [9] M. Vencelj *et al.* (unpublished).
 [10] J. Cederkäll *et al.*, *Phys. Rev. C* **53**, 1955 (1996).
 [11] J. Kownacki *et al.*, *Nucl. Phys.* **A627**, 239 (1997).
 [12] R. Machleidt, F. Sammarruca, and Y. Song, *Phys. Rev. C* **53**, R1483 (1996).
 [13] A. Holt, T. Engeland, M. Hjorth-Jensen, and E. Osnes, *Phys. Rev. C* **61**, 064318 (2000).
 [14] M. Hjorth-Jensen, T.T.S. Kuo, and E. Osnes, *Phys. Rep.* **261**, 125 (1995); T. Engeland, M. Hjorth-Jensen, and E. Osnes, *Phys. Rev. C* **61**, 021302(R) (2000).
 [15] G. Leander *et al.*, *Phys. Rev. C* **30**, 416 (1984).
 [16] J. Duflo and A.P. Zuker, *Phys. Rev. C* **59**, R2347 (1999).
 [17] M. Lipoglavšek *et al.*, *Phys. Rev. C* **65**, 021302(R) (2002).
 [18] D. Alber *et al.*, *Z. Phys. A* **332**, 129 (1989).
 [19] C. Fahlander *et al.*, *Phys. Rev. C* **63**, 021307(R) (2001).
 [20] A.R. Poletti *et al.*, *Phys. Rev. C* **10**, 2312 (1974).
 [21] N. Bendjaballah *et al.*, *Nucl. Phys.* **A280**, 228 (1977).